EARTHQUAKE ENGINEERING AND STRUCTURAL DYNAMICS
Earthquake Engng Struct. Dyn. 2000; **29**: 789–812

Dynamic loading test and simulation analysis of full-scale semi-active hydraulic damper for structural control

Naoki Niwa[1,*,†], Takuji Kobori[1,‡], Motoichi Takahashi[1,§], Hiroshi Midorikawa[2,¶], Narito Kurata[1,†] and Takayuki Mizuno[2,‖]

[1] *Kobori Research Complex, Kajima Corporation, KI Building, 6-5-30 Akasaka, Minato-ku, Tokyo 107-8502, Japan*
[2] *Industrial Facilities Engineering Department Engineering Division, Kajima Corporation, 2-7 Motoakasaka 1-Chome, Minato-ku, Tokyo 107-8388, Japan*

SUMMARY

A semi-active hydraulic damper (SHD) for a semi-active damper system, which is useful for practical structural control especially for large earthquakes, has been developed. Its maximum damping force is set to 1 or 2 MN, and it is controlled by only 70 W of electric power. An SHD with a maximum damping force of 1 MN was applied to an actual building in 1998. This paper first presents the results of a dynamic loading test to confirm the control performance of the SHD. Next, an analytical model of SHDs (SHD model) is constructed with the same concept for two kinds of SHDs based on the test results. Through simulation analyses of the test results using the proposed SHD model, the dynamic characteristics of the SHD can be well represented within practical conditions. Simulation analyses are also carried out using a simple structure model with the SHD model. It is shown that this SHD model can be used to precisely evaluate the control effect of the semi-active damper system and is useful in practical SHD design under the applied conditions. Copyright © 2000 John Wiley & Sons, Ltd.

KEY WORDS: semi-active hydraulic damper; full-scale model; dynamic loading test; analytical model; controller gain; dynamic characteristics

1. INTRODUCTION

The semi-active control system, which has been the subject of vigorous research and development, is a useful structural control system for large earthquakes because of its small electric power requirement [1]. In order to realize this system, a practical semi-active control device is required. Semi-active friction dampers [2], semi-active oil dampers [3], magnetorheological dampers [4] and electrorheological dampers [5] have been studied for this purpose. For practical application,

* Correspondence to: Naoki Niwa, Kobori Research Complex, Kajima Corporation, KI Building, 6-5-30 Akasaka, Minato-ku, Tokyo 107-8502, Japan.
† Senior Research Engineer
‡ Professor Emeritus of Kyoto University, Dr of Engng, Chief Executive Adviser, Kajima Corporation
§ Deputy Senior Manager, Kobori Research Complex
¶ Chief
‖ Assistant Chief

Received 7 October 1999
Revised 10 November 1999
Accepted 17 November 1999

a dynamic loading test is needed to confirm their control performance. In addition, to exactly confirm the control system's effectiveness, an appropriate analytical model is required specifically to express the dynamic characteristics of the control device. With respect to the analytical model, several types, such as the magnetorheological damper [6] and the semi-active oil damper [7,12] have been reported. For practical application of the actual control device, we must set up an appropriate analytical model to simulate the behaviours of a wide variety of objective structures. The analytical model must therefore be simple enough to simulate multi-degree-of-freedom models. However, utilization of such a simple and practical model has not yet been reported.

The authors reported a basic concept of the semi-active damper system and results of shaking table tests in 1991 [8]. Then, a scale model of a semi-active hydraulic damper (SHD) with a 200 kN maximum damping force was reported in 1992 [9]. Following these two studies, based on the results of a shaking table test using a 3-storey model structure [10] and an improved SHD [11], a simple analytical model of an SHD was proposed [9,11,12]. At the same time, based on a simulation analysis for high-rise buildings, the control performance of the SHD was confirmed, and we found that a maximum damping force of 1–2 MN was required for the actual control device [13]. Recently, full-size SHDs (1 MN SHD and 2 MN SHD) with a maximum damping force of 1 and 2 MN for large earthquakes have been designed, and their control performance confirmed by a dynamic loading test [14,15]. These SHDs can be controlled by only about 70 W of electric power; making them useful as practical devices for semi-active control systems. Based on these studies, a 1 MN SHD was applied to an actual building in 1998 [14,16].

This paper presents a dynamic loading tests performed to confirm the control performance of two kinds of SHDs. These tests comprise a sinusoidal loading test under simplified seismic response conditions and a seismic loading test under typical earthquake response conditions of buildings. They take into account controller gain characteristics, which are significant in evaluating the SHD's control performance. Next, an analytical model of the SHDs (SHD model) is created based on the same concept for two kinds of SHDs, and they precisely represent the SHD's dynamic characteristics. Because the SHD model is simple, it can be incorporated into the building structure model. It well simulated the test results in the wide frequency range within practical conditions, thus representing the SHD's dynamic characteristics. Furthermore, simulation analyses were carried out using a simple structure model with the SHD model. It is shown that the established SHD model is useful in precisely evaluating the control effect of the semi-active damper system and in designing a practical SHD under its applied conditions.

2. OBJECTIVE BUILDING

An SHD application method is shown in Figure 1(a). The SHDs are mainly installed between a brace and a beam in the buildings. Figure 1(b) shows the specification of the building with the SHDs. The objective buildings are four steel frame office buildings with first natural frequencies of 0.25–2.0 Hz. The individual floor heights are 4 m. The floor areas are determined in proportion to the total building height. The weight per unit area is assumed to be 8 kN/m^2. The stiffness distribution is determined on the basis of the design force according to the Japanese seismic design standards. The control effect for large earthquakes was studied based on the control simulation analysis for the objective buildings with SHDs [13]. The simulation results show that the damping force in buildings with first natural frequencies of 0.5–2.0 Hz is required to be 1 MN per SHD, and the damping force in buildings with first natural frequencies of 0.25–1.0 Hz is

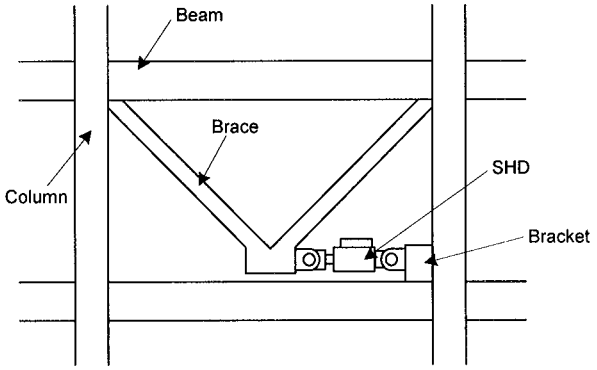

(a)Outline of frame installed SHD

(b)Objective building model

Item	Objective building model			
	0.5sec model	1sec model	2sec model	4sec model
Primary natural frequency(Hz)	2.00	1.00	0.50	0.25
Building height(m)	16	36	64	132
Number of floors	4	9	16	33
Floor area(m^2)	375	800	1500	3000
Weight of each floor(kN)	3000	6750	12000	24000
Number of SHD at each floor for one direction	2	2	2	4

Figure 1. Objective building specification.

required to be 2 MN per SHD. Therefore, the frequency range is set as 0.5–2.0 Hz for 1 MN SHD, and 0.25–1.0 Hz for 2 MN SHD.

3. SEMI-ACTIVE HYDRAULIC DAMPER

The SHD's hydraulic circuit, specification and outline are shown in Figure 2. It is composed of a double-rod cylinder, a piston-rod, a manifold, valves and a controller. It is connected with bolts to a brace and a bracket fixed at the column end through clevises on both sides, as shown in Figure 1(a). As a basic design philosophy, the SHD is designed to accurately produce the damping force (damping force command) calculated by any control law [9]. However, when the sign of the damping force command is opposite to that of the damping force generated by the SHD, or when a damping force is not to be produced, the opening of its flow control valve is increased so as not to generate a damping force.

3.1. Device configuration

The flow control valve is set in the connecting pipe between left and right cylinders. It controls the damping force by adjusting the oil flow. The flow control valve's mechanism is designed to

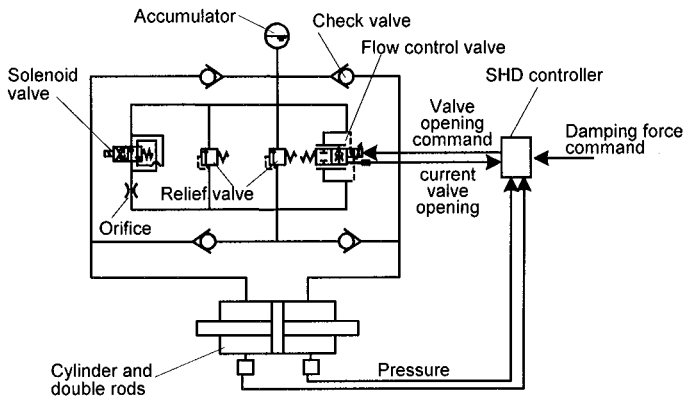

(a)Hydraulic circuit

(b)Specification of SHD

Item	1MN device	2MN device
Maximum damping force	1MN	2MN
Relief load	0.9MN	1.8MN
Maximum pressure	30MP	30MP
Allowable maximum velocity	25cm/sec	20cm/sec
Stroke	±6cm	±6cm
Stiffness	≧4MN/cm	≧8MN/cm
Maximum damping coefficient	2MNsec/cm	5MNsec/cm
Scale	W390×H750×L1650	W470×H870×L2315
Weight	13kN	23kN

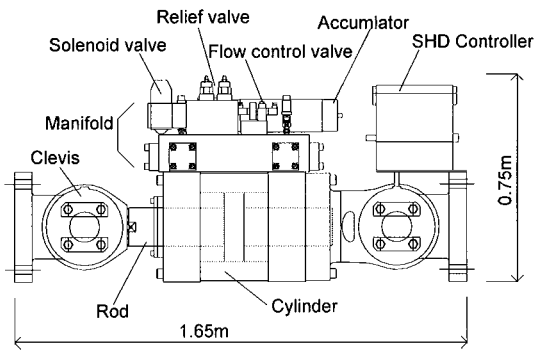

(c)Outline of 1MN device

Figure 2. Semi-active hydraulic damper.

conserve energy efficiently while controlling building responses. Thus, a two-stage valve is employed. The main valve opening is adjusted through its back pressure controlled by the pilot valve. This has the advantage of controlling the large damping force with only about 70 W of

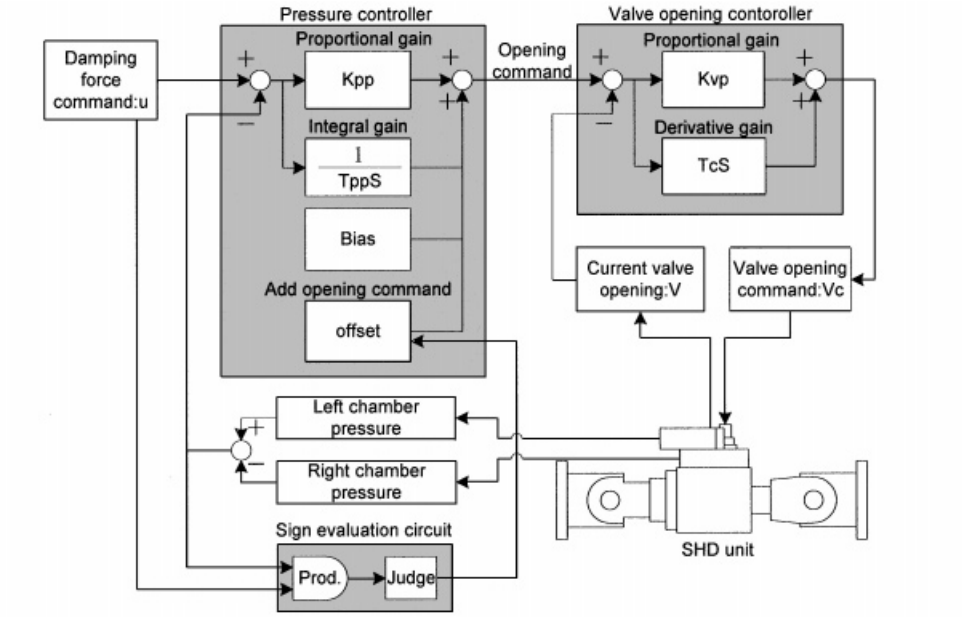

(a)SHD controller Configration

(b)Controller gain schedule

Gain name	Explanation	Gain type I	Gain type II
Kpp	Pressure controller proportional gain	0.94	1.953
Tpp	Pressure controller time constant(msec)	100	-
Bias	Pressure controller valve opening constant(%)	22	17～34
Offset	Pressure controller add valve opening(%)	80	80
Kvp	Valve opening controller proportional gain	2.34	3.125
Tc	Valve opening controller time constant(msec)	80	40

Figure 3. SHD controller.

electric power. Therefore, in case of power failure, the SHD can still function with a small uninterruptible power supply. In addition, the relief valve is installed in parallel with the flow control valve to prevent the SHD from generating the damping force above a relief load. Furthermore, as a fail-safe mechanism against the emergent event of a system or power failure, an emergency solenoid valve opens if the power is cut off. When it opens, the hydraulic oil flows through the orifice, thereby enabling the SHDs to function as passive dampers. The function of the accumulator is to provide initial pressure for the inner oil and to regulate the volume of the inner oil by temperature change and compression.

3.2. SHD controller

Figure 3(a) gives the configuration of the SHD controller. The function of the SHD controller is to control the pilot valve in the flow control valve when receiving the damping force command

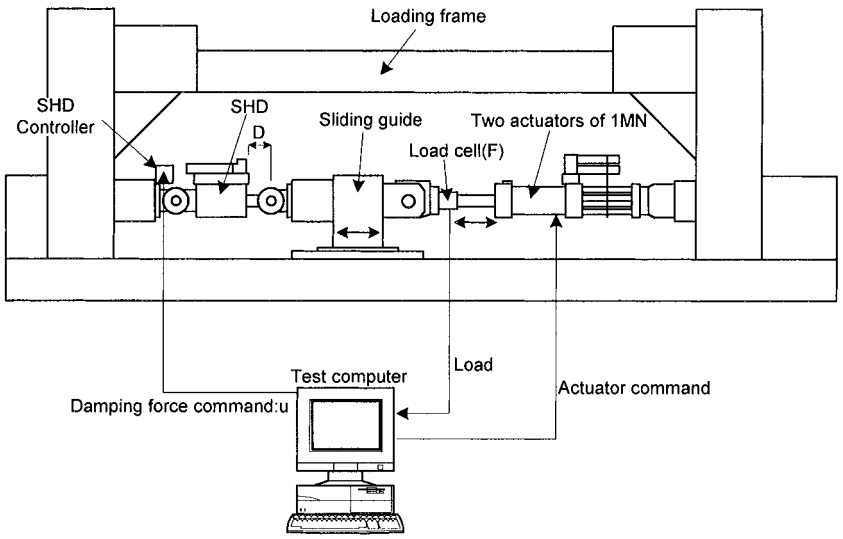

Figure 4. Test apparatus.

from the computer, and therefore to make the damping force accurately follow the command. It consists of a pressure controller, a valve opening controller and a sign evaluation circuit. The pressure controller's operation is based on the deviation between the command and the fed-back hydraulic pressure inside the cylinder through the pressure head. The valve opening controller's operation is based on the deviation between the fed-back current valve opening and the valve opening command from the pressure controller. The sign evaluation circuit increases the opening command in the pressure controller when the current damping force to be generated by the SHD and the command have opposite signs. Because of this function, the SHD does not generate the damping force for this occasion.

Figure 3(b) shows the composition of the controller gain mainly used in the dynamic loading test. The controller gain type I is adjusted for a sinusoidal loading with a frequency of 0.5 Hz on 2 MN SHD. The controller gain type II is adjusted for a sinusoidal wave loading with a frequency of 1.0 Hz for a 1 MN SHD. It is defined by varying the bias values via the pressures instead of the integral circuit.

4. DYNAMIC LOADING TEST METHOD

A dynamic loading test was performed for two kinds of SHDs to confirm their control performance. The tests comprised a sinusoidal loading test with simplified seismic response conditions and a seismic loading test under typical earthquake response conditions of buildings.

4.1. Test method

Figure 4 shows the test apparatus. The SHD was connected to two 1 MN actuators, which were attached to sturdy loading frames with a sliding guide. The measurement items were

the load generated by the actuators, i.e. F measured with a load cell, and the displacements of the SHD's cylinder rods, i.e. D. The dynamic loading test methods were of two types. One was a sinusoidal loading test to check the basic characteristics. The other was a seismic loading test to check the control performance under typical earthquake response conditions of the buildings.

4.1.1. Sinusoidal loading test. It was confirmed that the command required for the SHD during earthquakes was advanced 0–45° from the relative velocity between the cylinder and the rods (device velocity) [15]. In the sinusoidal loading test, the commands are given as simplified seismic response behaviours to confirm the basic control characteristics. The SHD's command amplitude was given in proportion to the amplitude of the device velocity. The following two loading cases were considered: (i) the command phase equal to the device velocity, (ii) the command phase given as 45° ahead of the device velocity. When the command was calculated, the constant value multiplied by the device velocity was defined as the damping coefficient.

4.1.2. Seismic loading test. The seismic loading test procedure was as follows: (i) the storey drift and the command pre-obtained in the seismic response analysis [13] of the objective buildings (as shown in Figure 1(a)) were inputted to the test computer; (ii) the command was transmitted directly to the SHD; and (iii) the deformation of the brace calculated by the actuator load was subtracted from the storey drift. The output of the evaluated displacements was then transmitted to the actuators as the displacement of the SHD. With this procedure, it is possible to evaluate the control performance of the SHD when it is installed in a building.

4.2. Test case

4.2.1. Sinusoidal loading test. Table I(a) shows the parameters of the sinusoidal loading test. Because its main purpose was to confirm the control performance by the flow control valve, the sinusoidal load was set up under the relief load. The parameters of the loading test for the 2 MN SHD were set up within the frequency range of 0.25–1.0 Hz. The maximum damping force commands, i.e. the U, were 500 and 1500 kN. The phase advances, i.e., the Ph of the commands for the device velocity, were 0 and 45°. The parameters of the loading test for the 1 MN SHD were set up within the frequency range of 0.5–2.0 Hz. The maximum damping force commands were 250 and 750 kN. The Ph were 0 and 45°. Then, comparing the case of frequency 1.0 Hz, maximum damping force command 250 kN, and Ph 0° for the controller gain type II, the changes in control performance were confirmed by the differences in the gain compositions and the damping coefficients, i.e., the C.

In addition, a controller gain variation test was carried out using the 1 MN SHD to study the effect on control performance. Their variations are shown in Table 1(b) based on the controller gain type II. The test parameters of the sinusoidal loading test were frequency 1.0 Hz, maximum damping force command 250 kN, damping coefficient 60 kN sec/cm and Ph 0°.

4.2.2. Seismic loading test. Table 1(c) shows the parameters of the seismic loading test. El Centro (1940 NS) with a normalized maximum velocity of 25 cm/sec was chosen as the input earthquake for the seismic response analysis. For the 2 MN SHD, a building with a primary natural frequency of 0.5 Hz was chosen as an example, because the median of the primary frequencies in the set of objective buildings was 0.5 Hz. A building with a primary natural frequency of 1.0 Hz

Table I. Parameters of the test.

(a)Parameters of sinusoidal loading test

Kind of device	Controller gain type	Frequency :f	Maximum damping force command:U	Damping coefficient:C	Phase advance:Ph
2MN device	Gain I	0.5Hz	500kN	500kNsec/cm	0°
					45°
			1500kN		0°
		1.0Hz	500kN	250kNsec/cm	
		0.25Hz		1000kNsec/cm	45°
1MN device		1.0Hz	250kN	125kNsec/cm	0°
					45°
			750kN		0°
		2.0Hz	250kN	50kNsec/cm	
		0.5Hz		250kNsec/cm	45°
					0°
	Gain II	1.0Hz	250kN	60kNsec/cm	0°
				200kNsec/cm	

(b)Parameters of controller gain variation test on sinusoidal loading test

Controller gain number	Pressure controller		Valve opening controller	
	Kpp	Bias(%)	Kvp	Tc(msec)
G1	1.953	17	3.125	40
G2		34		
G3	0.977	17～34		
G4	3.906			
G5	1.953		1.563	
G6			6.250	
G7			3.125	0
G8				128

Kind of device : 1MN device

Controller gain type : Gain II

Frequency : 1.0Hz

Maximum damping force command: 250kN

Damping coefficient : 60kNsec/cm

(c)Parameters of seismic loading test

Kind of device	Controller gain type	Earthquake	First period of building models	Story	Control law
2MN device	Gain I	El Centro 25cm/sec	2.0sec	1st	RFB
				12th	
				1st	AFB
1MN device			1.0sec	1st	RFB
				7th	
				1st	AFB

was chosen as an example for the same reason for the 1 MN SHD. Relative velocity feedback (RFB) and absolute velocity feedback (AFB) control based on the linear quadratic regulator theory were adopted to obtain the optimal damping force [13]. The first and middle floors were chosen as typical floors, because the pattern of the command required on each floor was considered.

5. ANALYTICAL SHD MODEL [17]

The analytical SHD model is created by the same concept for two kinds of SHDs. Because its composition is simple and it represents SHDs' dynamic characteristics, it can be useful in simulating the seismic response behaviour of the structure model.

5.1. Modelling concept

(a) The accumulator and the check valves are omitted, and the flow control valve with complicated non-linear characteristics is represented by a combination of the transfer functions. They facilitate its simulation using the structural model with the SHD model.

(b) The flow control valve functions define a physical meaning based on the specifications. Then, the SHD characteristic changes due to the specification change can be grasped without the dynamic loading test.

(c) The SHD controller is precisely represented. Then, the SHD characteristic changes due to the controller gain variations can be represented.

5.2. SHD model

Figure 5(a) shows the SHD model's composition. It is composed of a controller part, a flow control valve part and a cylinder part. In the analysis, the device velocity (V_{e1}) obtained from the test and the command (u) are inputted to the SHD model, and the analytical damping force (F) is outputted. As the device velocity in this analysis is obtained by differentiating the device displacement, which comprises deducting the displacement caused by the device stiffness from the relative displacement between cylinder and rod. The device stiffness is mainly determined by the compressibility of the inner oil in general. This stiffness value is pre-calculated based on the relationship between the load and displacement of the SHD. Figure 5(b) and (c) shows the specifications of the SHDs and the composition of the flow control valve.

(a) The controller model is precisely represented by the composition shown in Figure 3. It calculates a valve opening command (V_c) based on the command (u) from the computer, a current valve opening (V) and pressures (P) fed back from the SHD unit. The valve opening command (V_c) is outputted to a flow control valve model.

(b) The flow control valve model is represented by the composition shown in Figure 6(a). The valve opening command (V_c) from the controller is inputted to a pilot valve part represented by a linear transfer function [shown in Equation (1)], and then the pilot valve displacement (x_p) is outputted. Next, the relationship of pilot valve displacement (x_p) and pressure (P_{3p}) operating a main valve is represented by a first-order transfer function. The relationship among pilot valve displacement (x_p), flow (Q) and pressure (P_{3p}) is considered by an equivalent linear approximation based on a small value from the equilibrium state (x_{p0}, P_{3p0}). This is represented by the following

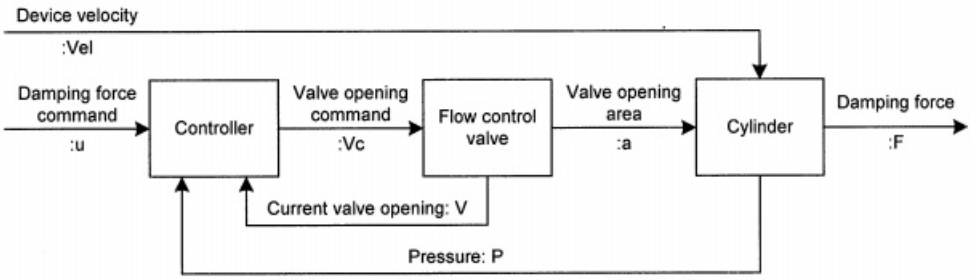

(a)Analytical device model

(b)Specification of device

Item		Symbol (unit)	1MN device	2MN device
Cylinder	Piston diameter	Dp(cm)	25	35.5
	Rod diameter	Dr(cm)	14	20
	area	A(cm^2)	336.9	675.6
Flow control valve (Main part)	Type	-	FE25C2X/315LV	
	valve diameter	Dm(cm)	2.2	
	area	Av(cm^2)	3.801	
	Weight	M (Nsec^2/cm)	1.45×10^{-3}	
	Viscous damping	Cv (Nsec/cm)	1.32	3.63
	Spring constant	Kv(N/cm)	10.8	58.6
	Initial disp.	xv_0(cm)	0.32	
	Maximum disp.	Xvmax(cm)	0.53	
Flow control valve (Pilot part)	Hole diameter	rp1(cm)	0.15	
	Volume	Vp(cm^3)	50	
	Maximum disp.	Xpmax (cm)	0.25	
Physical constant	Density	ρ (Nsec/cm^4)	8.702×10^{-7}	
	Flow constant	Cd	0.6	
	Bulk modulus	K (N/cm^2)	1.38×10^{5}	

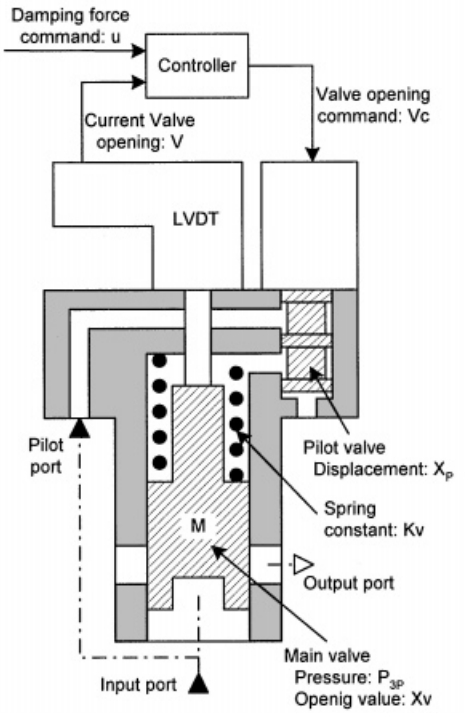

(c)Composition of flow control valve

Figure 5. Composition of analytical device model.

equation:

$$\frac{P_{3P}}{x_P}=\left(\frac{2P_{3P0}}{x_{P0}}\right)\frac{1}{\left(\dfrac{V_P\sqrt{2\rho\cdot P_{3P0}}}{KC_dEx_{P0}}\right)s+1}=\frac{X}{Ys+1} \tag{2}$$

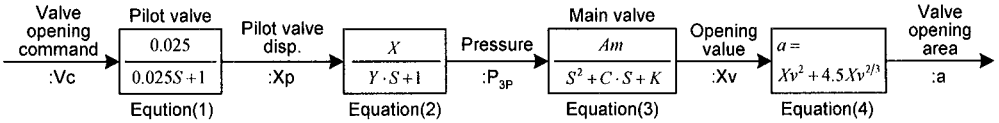

Current valve opening: $V = \dfrac{Xv}{Xv\max}$

(a)Flow control valve model

(b)Constant value of equation(2)

Kind of device	$X = \dfrac{2P_{3P0}}{x_{P0}}$			$Y = \dfrac{V_P\sqrt{2\rho \cdot P_{3P30}}}{K \cdot C \cdot E \cdot x_{P0}}$	
	Proposed value	Simulation value		Proposed value	Simulation value
1MN device	0.16~061	0.5Hz	0.25	$0.71\sim1.36\times10^{-3}$	1×10^{-3}
		1.0Hz	0.5		
		2.0Hz	0.8		
2MN device	0.84~3.34	0.25Hz	0.8	$1.62\sim3.24\times10^{-3}$	2×10^{-3}
		0.5Hz	1.2		
		1.0Hz	2.5		

(c)Constant value of equation(3)

Kind of device	Am(cm³/Nsec²)=Av/M	C(/sec)=c/M	K(/sec²)=k/M
1MN device	2620	900	7770
2MN device		2500	40404

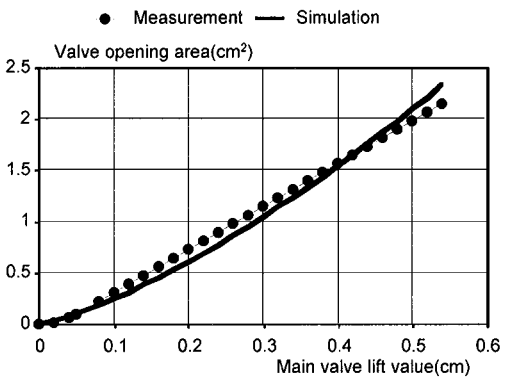

(d)Relationship between measured and simulation opening area of the main valve

Figure 6. Composition of flow control valve model.

where

$$X = \frac{2P_{3P0}}{x_{P0}}, \quad Y = \frac{V_P\sqrt{2\rho \cdot P_{3P0}}}{KC_dEx_{P0}}$$

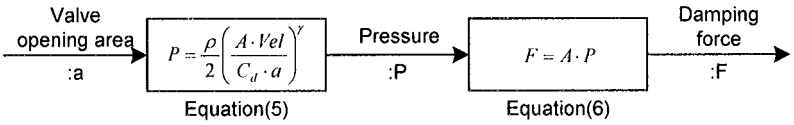

Kind of device	γ
1MN device	1.95
2MN device	1.80

Figure 7. Composition of cylinder model.

E is the ratio of the opening area for the pilot valve displacement. The other parameters are shown in Figure 5(b). The constant values are defined as shown in Figure 6(b), to consider the applied circumstances. Within these values, a time constant (Y) is established for the middle value in the simulation analysis, because it has a small variation and a small influence on the characteristic change. However, the gain constant (X) has a large variation and a large influence on the characteristics. Thus, it was determined as the simulation results agree with the test results. These constants set up together are shown in Figure 6(b). The main valve model is represented by a single-degree-of-freedom model [shown in Equation (3)] obtained from main valve area (A_v), valve mass (m), spring constant (k), and viscous damping (c) of the oil. The pressure (P_{3p}) is inputted, and the lift (X_v) of the main valve is outputted. The viscous damping (c) is set up by simulating the test results. Other parameters are used as the device specifications shown in Figure 5(b). The constants are shown in Figure 6(c). The lift value (X_v) normalized by the maximum lift value (X_{vmax}) is also fed back to the controller as a current valve opening (V). The valve opening area (a) corresponding to this lift value (X_v) is pre-obtained by a precise measurement of the main valve. Based on these relationships, the valve opening area (a) on the simulation is approximated by Equation (4) as shown in Figure 6(d).

Let us explicitly express the time delay of the flow control valve model. It is governed mainly by the transfer function of the pilot valve [Equation (1)] and that of the main valve [Equation (3)]. The time delay of the pilot valve is 25 msec, and that of the main valve is 130 msec for 1 MN SHD or 80 msec for 2 MN SHD, which are evaluated by the step response.

(c) Figure 7 shows the composition of the cylinder part model. The pressure (P) in the cylinder is calculated from Equation (5) based on the valve opening area (a) from the flow control valve model and the device velocity (V_{el}) obtained from the test. This pressure is also fed back to the controller. Then the damping force (F) is calculated by multiplying this pressure by the piston-area (A).

6. TEST AND ANALYTICAL RESULTS

This section discusses the test results and the analytical results by comparing the damping forces, the command, the test, and the SHD model proposed in Section 5.

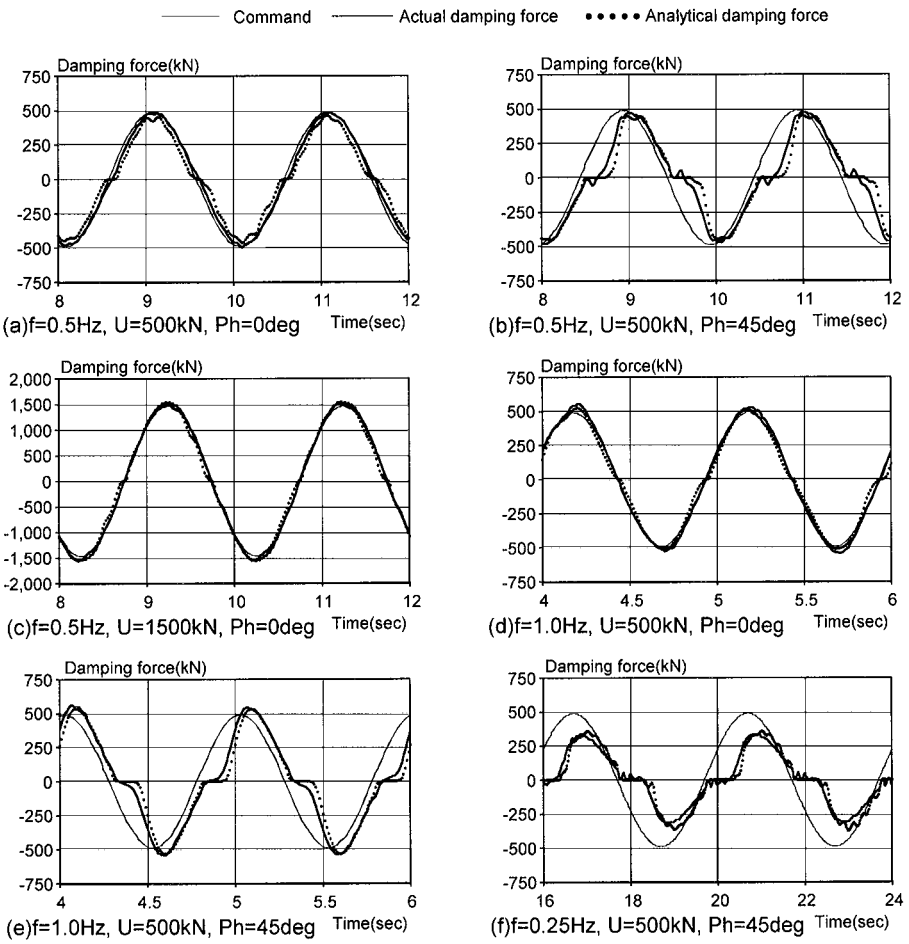

Figure 8. Results of sinusoidal loading test using 2 MN device.

6.1. Sinusoidal loading test

Figures 8(a)–(f) and 9(a)–(h) show the time histories of the damping force command and the damping force from the tests and the analyses for the 2 MN SHD and the 1 MN SHD, respectively. In addition, a controller gain variation test is presented for the five cases which show relatively large characteristic changes for gain variations on the controller gain type II. Figure 10(a)–(e) shows the time histories of the command and the damping force from the tests and analyses for the 1 MN SHD. The controller gain variation characteristics are considered by comparing these results with those of the controller gain type II shown in Figure 9(g).

(a) The test results are discussed. For the 2 MN SHD, the damping force generally follows the command well for a frequency of 0.5 Hz. For a frequency of 1.0 Hz, it has good control

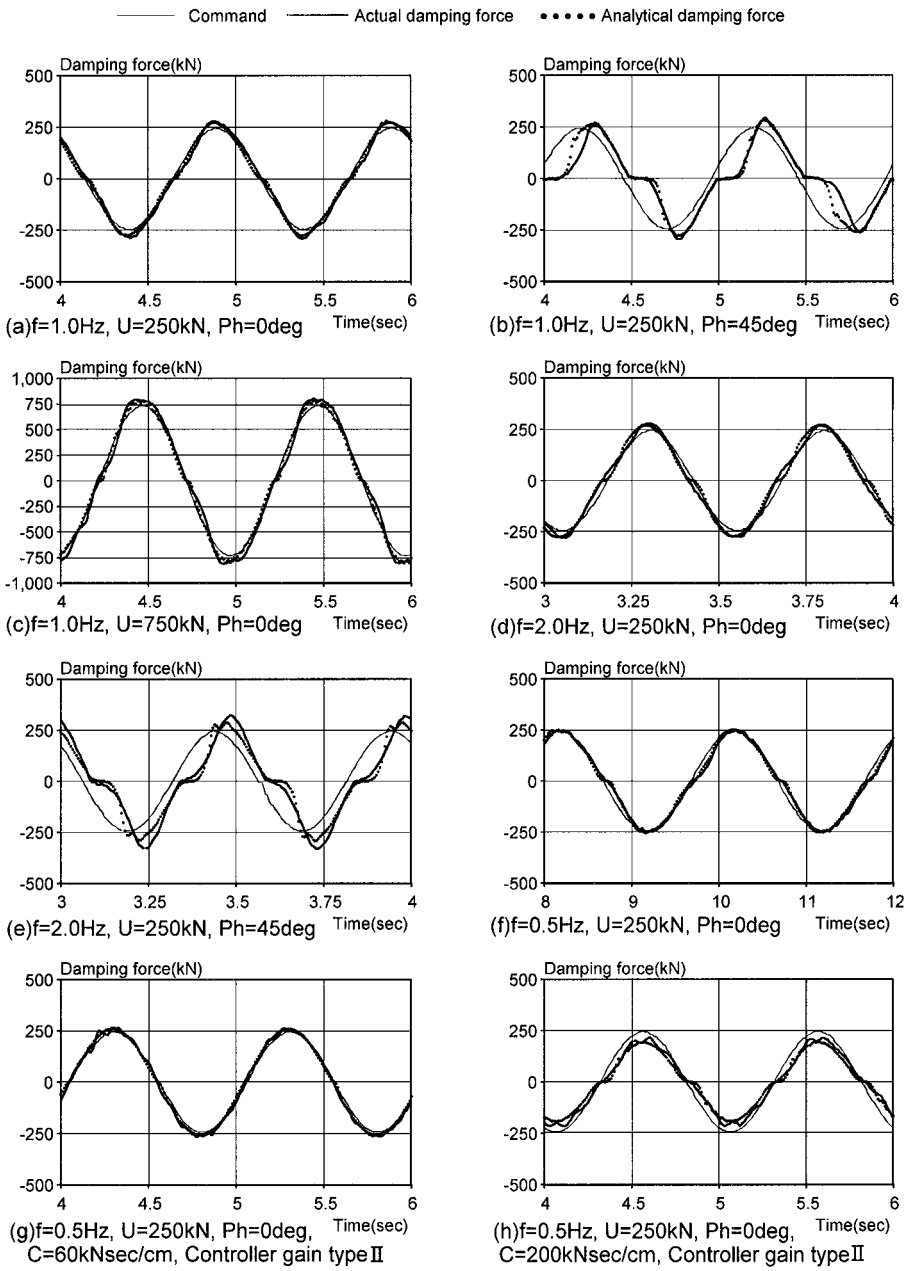

Figure 9. Results of sinusoidal loading test using 1 MN device.

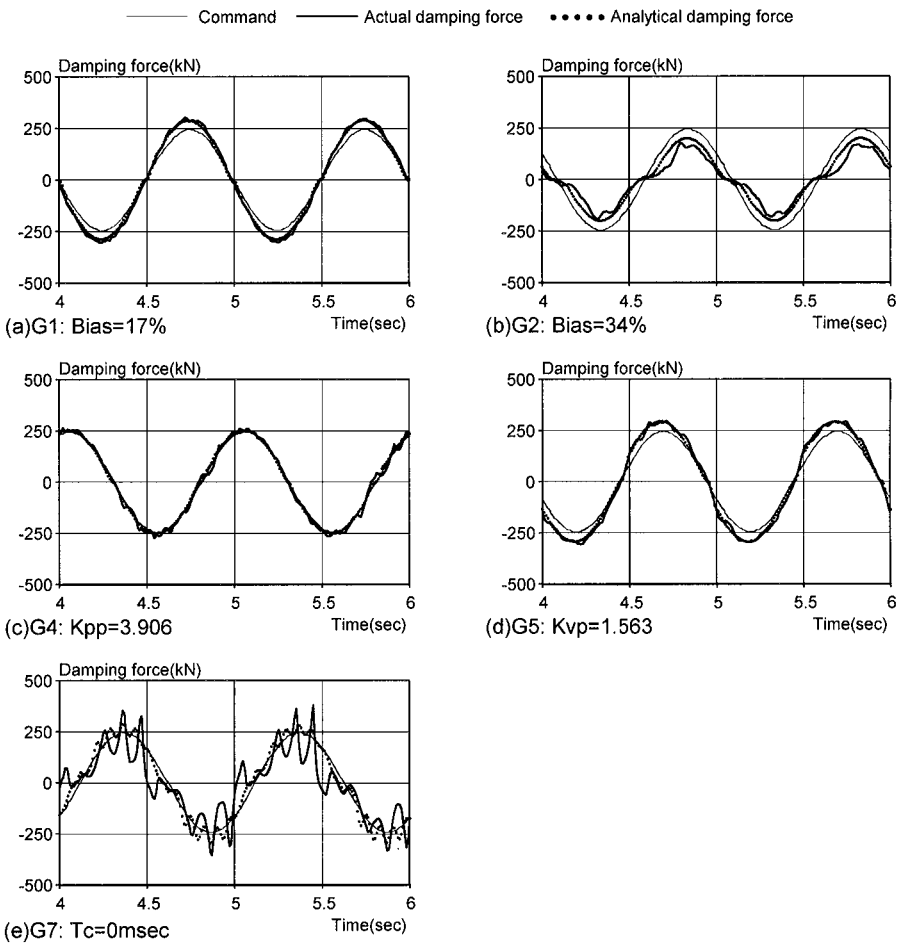

Figure 10. Results of controller gain change test using 1 MN device ($f = 1.0$ Hz, $U = 250$ kN, Ph $= 0°$).

performance for the phase 0°, but the damping force tends to over-shoot a little for the phase 45°. The damping force cannot follow the command for the frequency 0.25 Hz, because the proportional gains are small for this test case. The 1 MN SHD has good control performance for a frequency of 0.5 Hz, but the damping force tends to over-shoot a little for frequencies of 1.0 and 2.0 Hz. Furthermore, for the controller gain type II which is adjusted to a frequency of 1.0 Hz of the 1 MN SHD, the 1 MN SHD has good control performance for a damping coefficient of 60 kNsec/cm compared to the controller gain type I. However, for a damping coefficient of 200 kNsec/cm, the damping force tends to be small and not to follow the command, because the command is relatively large when the device velocity is small.

Next, the controller gain variation test is presented. As shown in Figure 10(a), when the pressure controller bias is small, the damping force is larger than the command because the valve

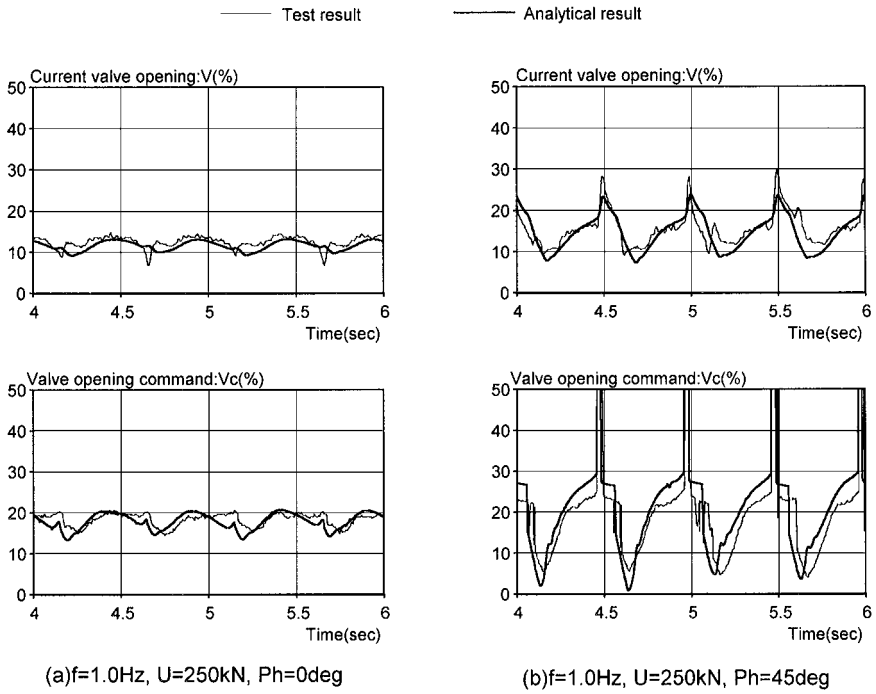

Figure 11. Valve opening of sinusoidal loading test results using 1 MN device.

opening is small. However, when the bias is large as shown in Figure 10(b), the damping force is smaller than the command. As shown in Figure 10(c), when the proportional gain of the pressure controller is large, the damping force tends to oscillate. As shown in Figure 10(d), when the proportional gain of the valve opening controller is small, the damping force is larger than the command because the current valve opening is behind the valve opening command. As shown in Figure 10(e), when the time constant of the pressure controller is 0, the damping force oscillates unstably because the valve opening command is delayed. These results demonstrate that the control performance of the SHD changes greatly depending on the controller gain values.

(b) The analytical results are discussed. For the 2 MN SHD, the analytical results represent the test results well, as shown in the following examples: (i) The damping force over-shoots for the command for a frequency of 1.0 Hz and a phase of 45°, (ii) The damping force tends to be small for the command for a frequency of 0.25 Hz and a phase of 45°. For the 1 MN SHD, the analytical results represent the test results well, as shown in the following examples: (i) using controller gain type I, the damping force tends to over-shoot for the command for a phase of 45° and frequencies of 1.0 and 2.0 Hz, (ii) using controller gain type II, the damping force for a damping coefficient of 200 kNsec/cm tends to be small and not to follow the command, unlike the case of a damping coefficient of 60 kNsec/cm.

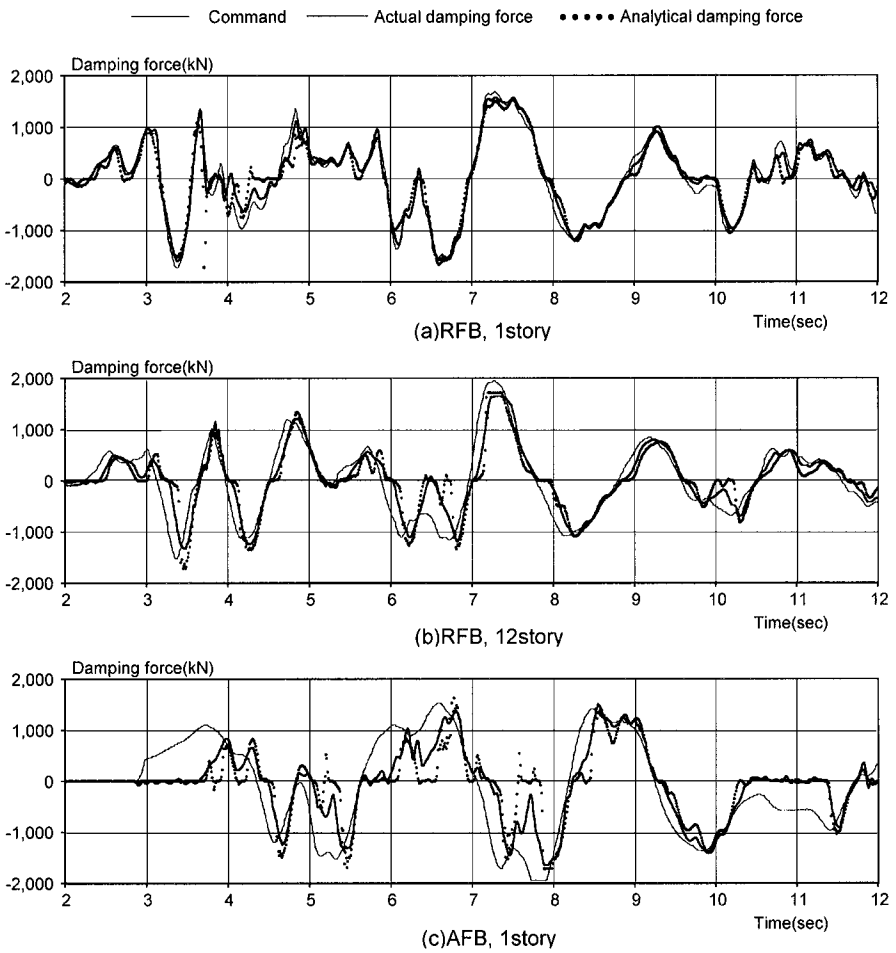

Figure 12. Results of seismic loading test using 2 MN device at 2 sec model.

Furthermore, Figure 11(a) and (b) shows the test results and analytical results of the valve opening command (V_c) outputted to the valve opening controller from the pressure controller, and the current valve opening (V). The analytical results of the SHD model simulate the test results well for the valve opening command (V_c) and the current valve opening (V), for example, an absolute value of the opening and the difference by phase advance. These results demonstrate that the SHD model well represents the test results regardless of the difference among frequencies, damping forces, phase advances, and damping coefficients.

Next, controller gain variation test is discussed. The analytical results represent the test results for the controller gain variations in all cases shown in Figure 10(a)–(e). These results show that the simulation of the SHD model agreed well with the test results for the control performance change by the controller gain variations.

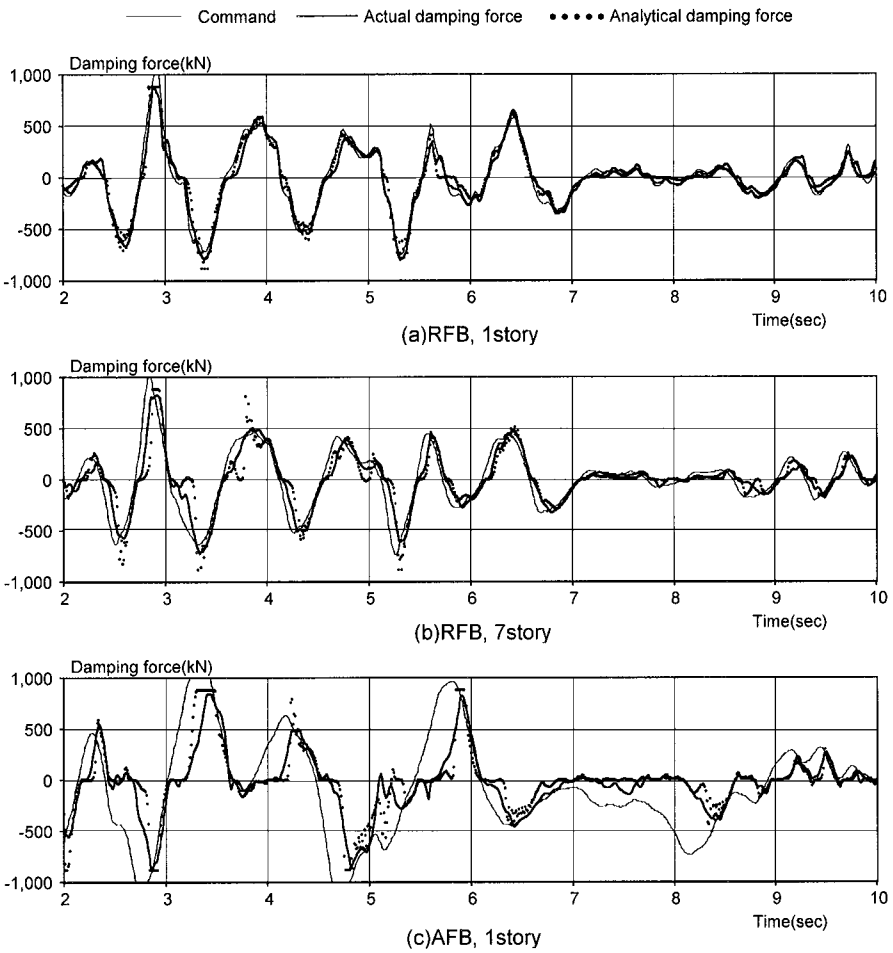

Figure 13. Results of seismic loading test using 1 MN device at 1 sec model.

6.2. Seismic loading test

Figures 12(a)–(c) and 13(a)–(c) show the time histories of the damping force command and the damping force from the tests and the analyses for the 2, and the 1 MN SHD, respectively.

(a) The test results are discussed. For the 2 and 1 MN SHDs, the damping force follows the command well for the first-floor response by the RFB. This is because the device velocity and the command generally have the same sign all the time. However, for the middle floor by the RFB and first floor by the AFB, no damping force can be generated for several durations by the operation of the sign evaluation circuit. This is because the command phase advances from the device velocity. This operation is an advantage of the semi-active device. Except for these timings, the test results of the SHDs show good control performance.

(b) The analytical results are discussed. For the 2 and 1 MN SHDs, the analytical results represent the test results well in all cases during the whole time history. Exceptionally, for the 2 MN SHD by the AFB on the first floor, no analytical damping force can be generated, and it does not fully follow the test result for nearly 6.4 and 7.7 sec. This is because the valve opening for the analysis does not agree well with the test one when the device velocity is small. However, this behaviour does not influence the control effect since the command is small during this timing. Thus, the proposed SHD model represents the test results well for the non-stationary control state during earthquakes.

7. RESPONSE ANALYSIS OF STRUCTURE WITH SHD MODEL

The simulation analysis is carried out using a simple structure model with an SHD model. It is shown that the established SHD model is useful in precise evaluation of the control effect of the semi-active damper system and in practical design of the SHD under its applied conditions.

7.1. Analytical conditions

7.1.1. Specifications. The SHD application method shown in Figure 1(a) is assumed. Figure 14(a) shows an analytical model for the simulation. The primary period of the main structure (M, K_f) is 1.0 second. The damping ratio is assumed to be 2 per cent. The sub-structure stiffness (k) including the device stiffness is chosen considering an actual building. The input wave is El Centro (1940 NS) with a normalized maximum acceleration of 10 cm/sec^2 to ensure that the device velocity is under the range confirmed in the test, and the damping force is under the relief load. One of the device models is the 1 MN SHD model constructed in Section 5. The other is an ideal device model which can be variable up to the maximum damping coefficient of 2 MNsec/cm verified by the test. The command to control the device is calculated by multiplying by the relative velocity of the main mass by the constant (control gain G).

7.1.2. Analytical cases

(a) *Influence of dynamic characteristics on control effect*. Figure 14(b) shows the parameters used in the analysis. The stiffness ratios (k/K_f) are 0.25, 0.5 and 1.0, and the control gains (G) are 5, 10, 20, 40 and 80. The applied device models are the 1 MN SHD model and the ideal model. The influence of dynamic characteristics on the control effect is considered by comparing the result of the SHD model with the result of the ideal model.

(b) *Study of the controller gain fitting under the applied conditions*. The response analysis is performed for the analytical condition shown in Figure 14(c) for the controller gain variations shown in Figure 14(d). Then the controller gains under the applied conditions are considered.

7.2. Analytical results

(a) *Influence of dynamic characteristics on control effect*. Figure 15(a) and (b) shows the maximum response acceleration through the analyses. The maximum response decreases as the control gain increases, shows its minimum at a certain value, then gradually increases. The response reduction effect was large when the sub-structure stiffness was large. Figure 15(c) shows the ratio of the SHD model's maximum acceleration to that of the ideal model. The acceleration

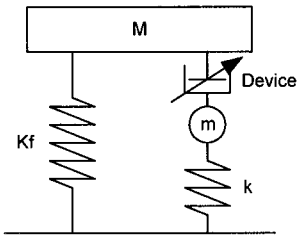

Period: T	1.0sec
Main mass: M	9800t
Sub mass: m	98t
Frame stiffness: Kf	3.92MN/cm

(a)Analytical model

(b)Analytical parameter 1

Device	1MN SHD model			Ideal model	
Input wave	El centro 10cm/sec^2				
Stiffness ratio: R=k/Kf	1.0		0.5		0.25
Control law	Relative velocity feedback				
Control gain: G	5	10	20	40	80

(c)Analytical parameter 2

Device	1MN analytical model
Input wave	El centro 10cm/sec^2
Stiffness ratio: R=k/Kf	1.0
Control law	Relative velocity feedback
Control gain: G	20

(d)Controller gain parameters

Controller gain number	Pressure controller				Valve opening controller	
	Kpp	Tpp(msec)	Bias(%)	Offset(%)	Kvp	Tc(msec)
g1	1.953	-	17～34	80	3.125	40
g2			17			
g3			34			
g4	0.977		17～34			
g5	3.906					
g6	1.953				1.563	
g7					6.250	
g8					3.125	0
g9						128

Figure 14. Analytical condition.

ratio is above 1.0 over the whole range due to the dynamic characteristics of the SHD model. This value changes from 0 to 30 per cent according to the stiffness ratios and control gains. These results demonstrate that the device's analytical model representing the dynamic characteristics is necessary to exactly estimate the response of the semi-active control system.

(b) *Study of the controller gain fitting under the applied conditions.* Figure 16 shows the analytical results of maximum acceleration ratios. The maximum acceleration response ratio is

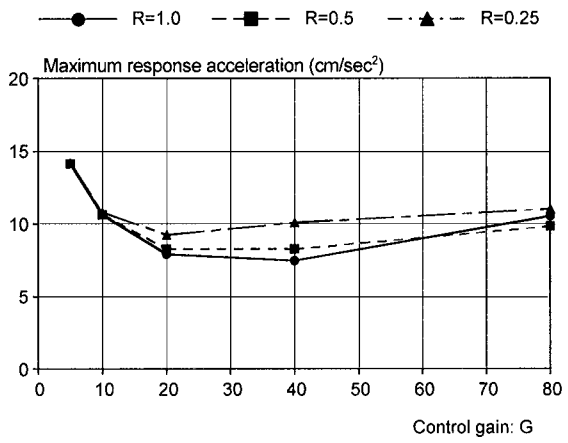

(a)Maximum response acceleration at ideal model

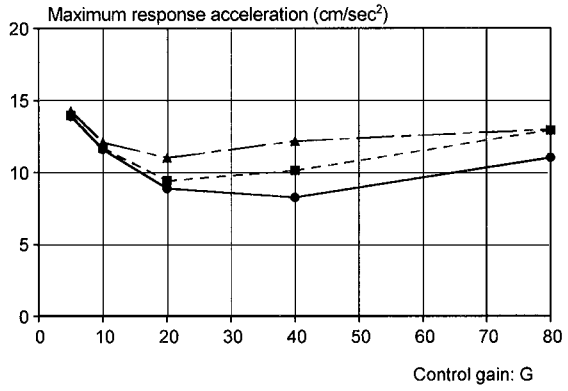

(b)Maximum response acceleration at 1MN SHD model

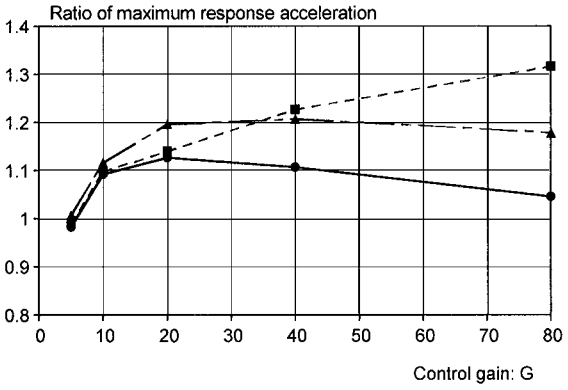

(c)Ratio of maximum response acceleration at 1MN SHD model per ideal model

Figure 15. Analytical results considered device dynamic characteristics.

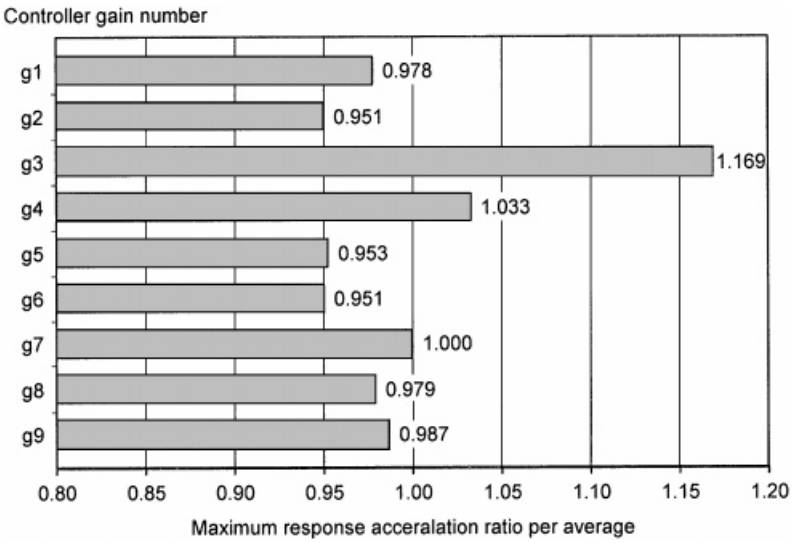

Figure 16. Analytical result controller gain parameters.

calculated for the average of all cases. The acceleration ratio changes according to the controller gain variations, and the gain numbers g_2 and g_6 indicate the best control effect from these results. These results show that these parametric analyses for the controller gain variations can determine an appropriate set of controller gains, which give the best control performance under the applied conditions.

8. CONCLUSIONS

The semi-active hydraulic damper (SHD) can control structural response during large earthquakes while consuming only a small amount of electric power. The control performance of SHDs was confirmed by a dynamic loading test. Next, the analytical model of the SHD was constructed, and the propriety of the SHD model was confirmed by simulating the test results. Furthermore, a simulation analysis was carried out using a simple structure model with an SHD model, and it confirmed the practical effectiveness of the SHD model. The following observations were made.

(1) Under the sinusoidal loading test, the basic characteristics of two kinds of SHDs (maximum damping force of 1 and 2 MN) were confirmed. With the same controller gain, the damping force tends to over-shoot when the excitation frequency is high, and the damping force decreases when the excitation frequency is low, because the deviation between the command and the damping force increases. For the same frequency, the damping force tends to be small compared to the command when the command becomes larger for a smaller device velocity (or for a large damping coefficient). The test results of the SHDs showed good control performance in the seismic loading

test under the actual applied conditions. It was also confirmed that the control performance of the SHD changed greatly depending on the controller gain values.

(2) The analytical SHD model was created based on the same concept on two SHDs. Because its composition is simple and it represents dynamic characteristics of the SHDs, it is useful to simulate the seismic response behaviour of the building structure model. The constructed SHD model simulated the sinusoidal loading test results well for the applied conditions of the SHDs. The SHD model also represented the seismic loading test and the controller gain variation test.

(3) Through the simulation analysis using a simple structure model with an SHD model, it was shown that the significance of using the SHD model was presented to exactly evaluate the response control effect on the system. Through the parametric response analysis using the SHD model with various controller gains, the appropriate controller gain can be designed under applied conditions.

These findings demonstrate that the control simulation analysis using the proposed SHD model is an effective design method for the semi-active damper system with the SHD.

ACKNOWLEDGEMENTS

The authors would like to express their gratitude to Messrs K. Ishii, Y. Matsunaga, J. Tagami and K. Nagai of Kajima Corporation for conducting the test and to Mr N. Shinohara of Kawasaki Heavy Industries Co., Ltd for manufacturing the SHD and constructing the SHD analytical model.

REFERENCES

1. Kobori T. Mission and perspective towards future structure control research. *Proceedings of the Second World Conference Structural Control*, vol. 1, Kyoto, JA, 1998; 25–34.
2. Hirai J. et al. Structural control with variable friction damper for seismic response. *Proceedings of the 11th World Conference on Earthquake Engineering*, Acapulco, Mexico, Paper No. 1934, 1996.
3. Patten WN. The I-35 Walnut Creek Bridge: an intelligent highway bridge via semi-active structural control. *Proceedings of the Second World Conference on Structural Control*, vol. 1, Kyoto, JA, 1998; 427–436.
4. Spencer Jr. et al. Smart dampers for seismic protection of structures: a full-scale study. *Proceedings of the Second World Conference on Structural Control*, vol. 1, Kyoto, JA, 1998; 417–426.
5. Gavin HP. et al. Control of structures using electrorheological dampers. *Proceedings of the 11th World Conference on Earthquake Engineering*, Acapulco, Mexico, Paper No.272, 1996.
6. Spencer Jr. et al. Phenomenological model for magnetorheological dampers. *Journal of Engineering Mechanics*, ASCE 1997; **123**: 230–238.
7. Patten WN. et al. Primer on design of Semiactive Vibration Absorbers (SAVA). *Journal of Engineering Mechanics*, ASCE 1998; **124**: 61–68.
8. Kobori T. et al. Research on active seismic response control system with variable structure characteristics — basic property of variable stiffness and damping mechanism and fundamental experiment by shaking table. *Journal of Structural Engineering* 1991; **37**B: 183–191.
9. Mizuno T. et al. Development of adjustable hydraulic damper for seismic response control of large structures. *Proceedings of the PVP Conference on PVP*-229, ASME, New Orleans, LA, 1992; 163–170.
10. Kurata N. et al. Shaking table experiment of active variable damping system. *Proceedings of the First World Conference on Structural Control*, Pasadena, CA, 1994; 2 (TP2): 108–117.
11. Mizuno T. et al. Adjustable hydraulic damper for seismic response control of large structures–development of damping force controller and dynamic loading test. *Transactions of the Journal of Society of Mechanical Engineers* 1993; **59**(566(c)): 3013–3020.
12. Kurino H. et al. Development and modeling of variable damping unit for active variable damping system. *Proceedings of the 11th World Conference on Earthquake Engineering*, Acapulco, Mexico, Paper No. 1521, 1996.
13. Kurata N. et al. Active variable damping system in large earthquakes. *Proceedings of the Third International Conference on Motion and Vibration Control*, vol. 3, Chiba, Japan, 1996, 285–290.

14. Niwa N. et al. Application of semi-active damper system to an actual building. *Proceedings of the Second World on Conference Structural Control*, vol. 1, Kyoto, JA, 1998; 815–824.
15. Matsunaga Y. et al. Dynamic loading test of actual size variable hydraulic damper. *Proceedings of the PVP Conference on PVP*-364, ASME, Denver, CO, 1998; 219–226.
16. Niwa N. et al. Application of semi-active hydraulic damper to an actual building. *Proceedings of the Fourth International Conference on Motion and Vibration Control*, Zurich, Switzerland, 1998; 607–612.
17. *Hydraulics and Pneumatics Hand Book*. The Japan Hydraulic and Pneumatics Society, 1989.

